

CFD Simulation and Optimization of Factors Affecting the Performance of a Fluidized Bed Dryer

Nazghelichi, Tayyeb

Department of Agrotechnology, College of Abouraihan, University of Tehran, Pakdasht, I.R. IRAN

Jafari, Arezou*⁺

Department of Chemical Engineering, Tarbiat Modares University, Tehran, I.R. IRAN

Kianmehr, Mohammad Hossein

Department of Agrotechnology, College of Abouraihan, University of Tehran, Pakdasht, I.R. IRAN

Aghbashlo, Mortaza

Department of Agricultural Machinery Engineering, Faculty of Agriculture Engineering and Technology, University of Tehran, Karaj, I.R. IRAN

ABSTRACT: *Computational Fluid Dynamics (CFD) is a computational technology that enables researchers to study the dynamics of things that flow. By using CFD, it is possible to build a computational model that represents a system under study. It not only predicts fluid flow behavior, but also the transfer of heat, mass, phase change, chemical reaction, mechanical movement, and stress or deformation of related solid. In this study, hydrodynamics behavior of a laboratorial fluidized bed dryer containing carrot cubes as well as heat transfer in the dryer was simulated using CFD. In addition, to understand the energy utilization the system was optimized using the Taguchi technique. Simulations were planned based on L₉ orthogonal array of Taguchi, and they were conducted at inlet air temperatures 50, 60 and 70 °C, bed depths 3, 6 and 9 cm and carrot cube dimensions 4, 7 and 10 mm. Results show that cube size and bed depth have the maximum and minimum contribution on the energy utilization ratio, respectively. According to the results inlet air temperature 70°C, cube size 4mm and bed depth 9cm were obtained as optimum conditions. Finally, a verification test was performed to confirm the validity of the used statistical method.*

KEY WORDS: *CFD simulation, Fluidized bed dryer, Optimization, Taguchi technique.*

INTRODUCTION

Carrot (*Daucuscarota L.*) is one of the important vegetables grown throughout the world containing high amounts of sugar [1] and it is known for its nutrient

contents besides appreciable amounts of B1, B2, B6 and B12 vitamins and minerals [2]. Carrot is cooked, dried to be used in instant soups or meals or consumed as raw.

* To whom correspondence should be addressed.

+ E-mail: ajafari@modares.ac.ir

1021-9986/13/4/81

12/\$/3.20

Carrots are the highest carotene containing foods which makes dried carrot slices an excellent candidate for developing an oil free snack food [1].

Drying of fruit and vegetables is a subject of considerable importance for their preservation and storage [2]. Dried fruits and vegetables have a longer shelf life, which makes it possible to use them in different products. In most industrial processes at least one drying step exists, which means the removal of relatively small amounts of water or other liquid from the solid material to reduce the content of residual liquid to an acceptable low value. Various methods of drying have been developed for solids, and each method has its own characteristics [3]. Considering the thermal efficiencies of the drying process, fluidized bed dryers are extensively used in particulate foods drying because they ensure high intensities of heat and mass transfer accompanied by high rates of drying. Fluidized-bed dryer has found many applications in chemical, metallurgical and pharmaceutical industries. They have also been investigated as a potential method for obtaining high quality dried foodstuffs, including fruit, vegetables and grain [4].

It has become apparent in recent years that energy resources, especially natural gas and oil, are limited [5]. In practical applications drying is a process that requires high energy input because of latent heat of water evaporation and relatively low energy efficiency of industrial dryers [6]. Energy consumption in drying ranges from a low value of under 5% for the chemical process industries to 35% for the papermaking operations. The major costs for dryers are in their operation rather than in their initial investment costs and thus new ideas in drying methods and dryer design are required to optimize energy consumption [5] as well as operating conditions.

In its most general meaning, optimization is the effort and process of making a decision, a design, or a system as perfect, effective, or functional as possible [7]. Process optimization has always been a noble objective of engineers entrusted with the responsibility for process development and improvement throughout the food industry [8]. There are some methods for optimization of food processes that each method has its own characteristics.

Taguchi techniques with analysis of variance (ANOVA) are statistical methods primarily developed by *Genichi Taguchi* to improve the quality of manufactured

goods. It is potentially beneficial for determining the most desirable design of products, best parameters combination for processes and optimization processes. In addition, experiment can be performed with the minimum replication using the orthogonal arrays [9]. Estimation of temperature amounts and its distribution inside the fluidized bed dryer is very important and necessary for calculation of energy and exergy efficiencies and thus for design objectives.

The complexity of the fluid dynamics problem makes it difficult or impossible to exactly solve for equations of an object in a flow [10]. Computational fluid dynamics is a branch of fluid mechanics that uses numerical methods and algorithms to solve and analyze problems that involve fluid flows. Computers are used to perform the calculations required to simulate the interaction of liquids and gases with surfaces defined by boundary conditions. CFD is a fast growing technology that can be useful to obtain shorter product-process development cycles, to optimize energy requirements, to optimize existing processes and to efficiently design new products and processes [11]. CFD models have been significantly enhanced and calculation speeds have greatly increased, so that CFD has been used to simulate hydrodynamics in complex flows such as two-phase flow in packed beds [10], fluidized beds [12], stirred tank reactors [13] or flash calculations [14].

Recently, some studies on the optimization of food processes were done [15-25]. However, less work has been done on the CFD simulation and optimization of fluidized bed drying parameters using Taguchi technique. In addition, effect of particle size and bed depth on energy utilization of fluidized bed drying of moist material such as fruits and vegetables is not understood well.

Therefore, in this research a fluidized bed dryer has been simulated using CFD techniques, and the focus of the work was on optimization of parameters that have effect on the system such as particle size, bed depth and drying air temperature using Taguchi technique.

EXPERIMENTAL SECTION

Experimental set-up

In this study a laboratorial fluidized bed dryer, developed in the "Agricultural Technical Engineering Laboratory" in College of Abouraihan (University of Tehran, Iran) was investigated. Fig. 1 illustrates the

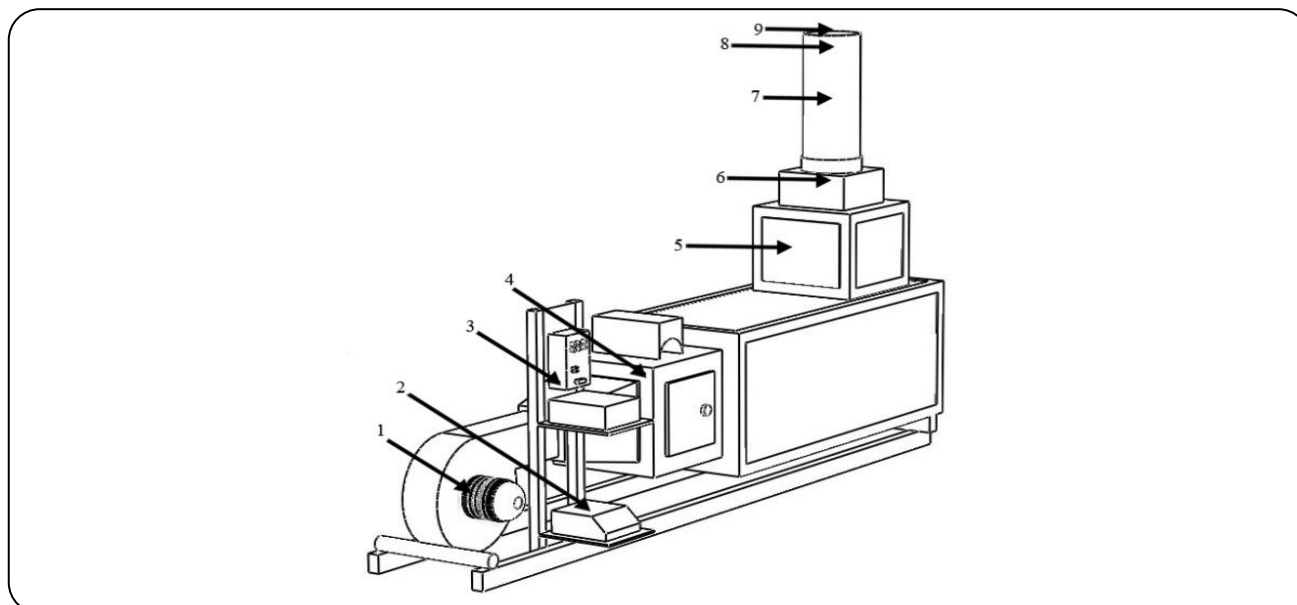


Fig. 1: Schematic view of the experimental equipment: blower (1); inverter (2); heaters control unit (3); heaters (4); chamber (5) thermocouple (6-8); fluidization cylindrical chamber (7) anemometer (9).

schematic view of experimental equipments. The Plexiglas cylindrical chamber has diameter 150 mm and height 300 mm. A centrifugal blower provided an air supply, drawn from ambient air. In order to supply the required airflow rate for fluidization of carrot cubes, the blower speed was changed by an inverter which operated directly on the blower motor. The dryer had an automatic temperature controller with an accuracy of $\pm 1^\circ\text{C}$. Air velocity was measured using an anemometer (PROVA AVM-07 TES, Co., Taipei, Taiwan) with an accuracy of ± 0.05 m/s. Fresh carrots were obtained from a local market in Pakdasht, Iran and stored in a refrigerator at about 5°C . At the start of each experiment carrots were washed and cut into cubes manually, having dimensions of $4\times 4\times 4$, $7\times 7\times 7$ and $10\times 10\times 10$ mm. The initial moisture content of the carrot was determined by drying of 50 g of sample in an oven at $105 \pm 2^\circ\text{C}$. In this study the ambient temperature and environment air relative humidity were taken as, $T_\infty = 25^\circ\text{C}$ and $\phi = 20\%$, respectively. The initial moisture content of the carrots was observed to be $89.3 \pm 0.36\%$ (kg water/ kg dry matter).

Simulated geometry

As the cylindrical drying chamber is the most important part, it has been simulated in this work. To save the computational time and cost, the symmetric cylinder was created as the drying chamber. In order to

generate the geometry and grid, commercial software, Gambit 2.3.16 was used.

Results are grid independent. A grid independency check has been performed, and the outlet air velocity magnitude at inlet air temperature 50°C , cube size 10 mm and bed depth 6 cm was considered to compare different grids. Results have been shown in Table 1. As the difference between numerical results in grid 2 and 3 is less than 0.1%, so to save cost and time grid 2 has been chosen for all tests.

THEORITICAL SECTION

Governing equations

The governing equations are as follow:

The equation for conservation of mass, or continuity equation, is:

$$\frac{\partial \rho}{\partial t} + \nabla \cdot (\rho \vec{v}) = 0 \quad (1)$$

Conservation of momentum has been described by:

$$\frac{\partial}{\partial t} (\rho \vec{v}) + \nabla \cdot (\rho \vec{v} \vec{v}) = -\nabla p + \nabla \cdot (\bar{\tau}) + \rho \vec{g} \quad (2)$$

The stress tensor $\bar{\tau}$ is given by:

$$\bar{\tau} = \mu \left[(\nabla \vec{v} + \nabla \vec{v}^T) - \frac{2}{3} \nabla \cdot \vec{v} \mathbf{I} \right] \quad (3)$$

Table 1: Air outlet velocity magnitude at different grids.

Grid	1	2	3
Number of elements	3×10^4	3×10^5	5.3×10^5
Number of nodes	1.2×10^4	8.7×10^4	1.4×10^5
Outlet velocity (m/s)	2.38	3.63	3.64

The second term on the right hand side shows the effect of volume dilation.

The energy equation is:

$$\frac{\partial}{\partial t}(\rho E) + \nabla \cdot (\bar{\vartheta}(\rho E + p)) = \nabla \cdot \left[k_{\text{eff}} \nabla T - \sum_j h_j \bar{J}_j + \bar{\tau}_{\text{eff}} \cdot \bar{\vartheta} \right] + S_h \quad (4)$$

k_{eff} is the effective conductivity ($k+k_t$, where k_t is the turbulent thermal conductivity, defined according to the turbulence model being used). The first three terms on the right-hand side of the Eq. (4) represent energy transfer due to conduction, species diffusion, and viscous dissipation, respectively. S_h includes the heat of chemical reaction, and any other defined volumetric heat sources.

In Eq. (4):

$$E = h - \frac{p}{\rho} + \frac{\vartheta^2}{2} \quad (5)$$

where the sensible enthalpy, h , for ideal gases is defined as:

$$h = \sum_j Y_j h_j \quad (6)$$

In Eq. (6), Y_j is the mass fraction of species j and:

$$h_j = \int_{T_{\text{ref}}}^T C_{p,j} dT \quad (7)$$

where T_{ref} , is 298.15°K.

The species transport equation is:

$$\frac{\partial \rho Y}{\partial t} + \nabla \cdot (\rho \bar{\mathbf{v}} Y) = -\nabla \cdot \bar{J}_W \quad (8)$$

where Y is the water mass fraction and \bar{J}_W , the water mass flux, defined as:

$$\bar{J}_W = -\rho D_{\text{eff}} \nabla Y \quad (9)$$

where D_{eff} is the water effective diffusivity.

Turbulence Model

The realizable k - ϵ model has been chosen as the turbulence model. Transport equations for k and ϵ are:

$$\frac{\partial}{\partial t}(\rho k) + \frac{\partial}{\partial x_i}(\rho k u_i) = \frac{\partial}{\partial x_j} \left[\left(\mu \frac{\mu_t}{\sigma_k} \right) \frac{\partial k}{\partial x_j} \right] + G_k + G_b - \rho \epsilon - Y_M + S_k \quad (10)$$

and

$$\frac{\partial}{\partial t}(\rho \epsilon) + \frac{\partial}{\partial x_i}(\rho \epsilon u_i) = \frac{\partial}{\partial x_j} \left[\left(\mu + \frac{\mu_t}{\sigma_\epsilon} \right) \frac{\partial \epsilon}{\partial x_j} \right] + \rho C_{1\epsilon} S_\epsilon - \rho C_{2\epsilon} \frac{\epsilon^2}{k + \sqrt{v\epsilon}} + C_{1\epsilon} \frac{\epsilon}{k} C_{3\epsilon} G_b + S_\epsilon \quad (11)$$

where:

$$C_{1\epsilon} = \max \left[0.43, \frac{\eta}{\eta + 5} \right] \quad (12)$$

$$\eta = S \frac{k}{\epsilon} \quad (13)$$

$$S = \sqrt{2 S_{ij} S_{ij}} \quad (14)$$

In the above equations, G_k represents the generation of turbulence kinetic energy due to the mean velocity gradients. G_b is the generation of turbulence kinetic energy due to buoyancy. Y_M shows the contribution of the fluctuating dilatation in compressible turbulence to the overall dissipation rate. σ_k , σ_ϵ , $C_{2\epsilon}$ and $C_{1\epsilon}$ are constants and established to ensure that the model performs well for certain canonical flows. Constant values are represented in Table 2. S_k and S_ϵ are source terms, and in the present work they were assumed zero.

The degree to which ϵ is affected by the buoyancy is determined by the constant $C_{3\epsilon}$:

$$C_{3\epsilon} = \tanh \left| \frac{\hat{u}}{u} \right| \quad (15)$$

Table 2: Constants in the turbulence model.

$C_{1\varepsilon}$	$C_{2\varepsilon}$	σ_k	σ_ε
1.44	1.92	1	1.3

Table 3: The various parameters selected and their respective levels.

Factors	Level 1	Level 2	Level 3
A: Bed depth	3cm	6cm	9cm
B: Cube size	4mm	7mm	10mm
C: Inlet air temperature	50°C	60°C	70°C

Energy Utilization

Thermodynamic analysis has appeared to be an essential tool for optimization and design of thermal systems. Energy utilization is the proportion of energy supplied to the fluidization chamber for drying of wet materials. Energy utilization ratio has been defined as the ratio of energy utilization to the useful energy given from heater [26]. Thus the energy utilization ratio is a proper dimensionless term and has been used as the objective function for optimization of the system.

Energy utilization can be calculated by applying the first law of thermodynamics [27]:

$$Eu = \dot{m}_{da} (h_{dai} - h_{dao}) \quad (16)$$

The mass flow rate of the air, \dot{m}_{da} , can be calculated using the following equation [26, 28]:

$$\dot{m}_{da} = \rho_a V_a A_{dc} \quad (17)$$

The enthalpy of drying air can be determined as follow [29]:

$$h_{da} = C_{pda} (T - T_\infty) + h_{fg} w \quad (18)$$

The specific heat of inlet and outlet air, C_{pda} , was obtained by [29]:

$$C_{pda} = 1.004 + 1.88w \quad (19)$$

The below equation can be used to transform the relative humidity to humidity ratio of the air [26, 29-33]:

$$w = 0.622 \frac{\phi P_{vs}}{P - P_{vs}} \quad (20)$$

Humidity ratio of outlet air is calculated by [31]:

$$w_{dao} = w_{dai} + \frac{DR}{\dot{m}_{da}} \quad (21)$$

The (DR) has been defined as:

$$DR = \frac{W_t - W_{t+\Delta t}}{\Delta t} \quad (22)$$

The Energy Utilization Ratio (EUR) of drying chamber is calculated using the following equation [29]:

$$EUR = \frac{\dot{m}_{da} (h_{dai} - h_{dao})}{\dot{m}_{da} (h_{dai} - h_e)} \quad (23)$$

Numerical method

The computations were performed by commercial software, Fluent. The second order upwind discretization scheme was used to solve continuity, momentum, and energy equations. The pressure-velocity coupling has been obtained using SIMPLE algorithm. The initial temperature in the system was adjusted equal to ambient temperature 298 K. Boundary conditions of mass flow inlet and pressure outlet were applied for the bottom and top of the dryer, respectively. The side walls were insulated and no slip velocity was assumed. Turbulence predictions for the system were obtained using the realizable k- ε model.

Orthogonal array and simulation parameters

For Taguchi design and subsequent analysis, the software named Qualitek-4 (Version 4.82.0) was used. The appropriate orthogonal array, L9, for the simulation was determined by the software. This means that 9 simulations with different combinations of the factors should be conducted in order to study the main effects and interactions. As Table 3 shows in this work the effect of three parameters on energy utilization ratio at three levels have been studied. Taguchi L9 orthogonal array of the simulations designed are shown in Table 4.

Table 4: Taguchi L9 orthogonal array design.

Simulation number	A	B	C
1	1	1	1
2	1	2	2
3	1	3	3
4	2	1	2
5	2	2	3
6	2	3	1
7	3	1	3
8	3	2	1
9	3	3	2

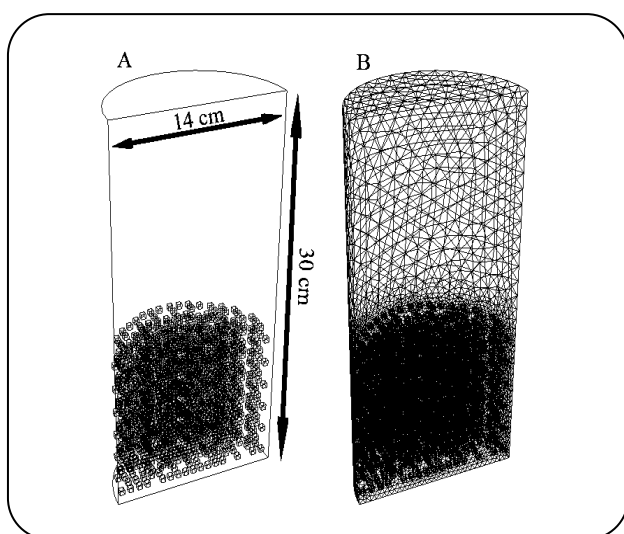


Fig. 2: (a) Schematic of the geometry used in this study. Here, bed depth and cubic carrot size are 9cm and 4mm, respectively; (b) The generated grid by the size function.

RESULTS AND DISCUSSION

The schematic of the geometry and the grid used in simulations, have been illustrated in Fig. 2. As it can be seen in Fig. 2, the carrot cubes were randomly scattered in all over the specified height of bed. All Taguchi tests were performed and energy utilization ratio was calculated. The results have been displayed in Table 5.

Temperature is the most important parameter that can be measured at every point inside the drying chamber for calculation of energy utilization at those points. Fig. 3 represents temperature contours of the drying chamber at different times. The hot drying air, crossing upward throughout the fluidization chamber, has lower amount of temperature toward the top of cylinder because of heat transfer from air to carrot cubes. All the simulations have

been conducted to reach the stable condition and thus at the end of the process, temperature of the entire cylinder was near the inlet air temperature.

In order to investigate the temperature distribution along the cylinder more accurately, the height of drying chamber has been divided to some layers (Fig. 4), and the temperature has been estimated in each layer. Fig. 5 displays variations of temperature versus time and surface position. As can be seen in Fig. 5, the temperature of first surface in the bottom of drying chamber was equal to the inlet air temperature in the first time step. Temperature of surfaces was decreased with increasing the height of the surfaces along the drying chamber and it became equal to ambient temperature at the top of drying chamber. With passing time, temperature of lower surfaces became equal to the inlet air temperature, and upper surfaces became warmer than the ambient temperature until the whole chamber reached the stable condition at the end of process.

Drying is a time-dependent simultaneous process of mass and heat transfer. Therefore, these transport phenomena were simulated simultaneously in this work. Fig. 6 represents the results of water diffusion inside the carrot cubes.

In Fig. 6 (a) and (b) volume fraction of water in a carrot cube was represented in two different times for cube size 10 mm, air velocity 4 m/s and bed depth 90 mm. As mentioned earlier, the initial moisture content of carrot cubes was observed to be $89.3 \pm 0.36\%$ (kg water/kg dry matter) and about 75% of initial moisture content would be lost at the end of drying period in every experimental drying condition. As Fig. 6 (a) and (b) illustrate, the amount of water inside carrot cubes decreases with passing time. Fig. 6 (c) shows water vectors that

Table 5: Energy utilization ratio in Taguchi tests.

Simulation Number	Energy utilization ratio
1	0.113
2	0.098
3	0.073
4	0.164
5	0.116
6	0.047
7	0.214
8	0.111
9	0.066

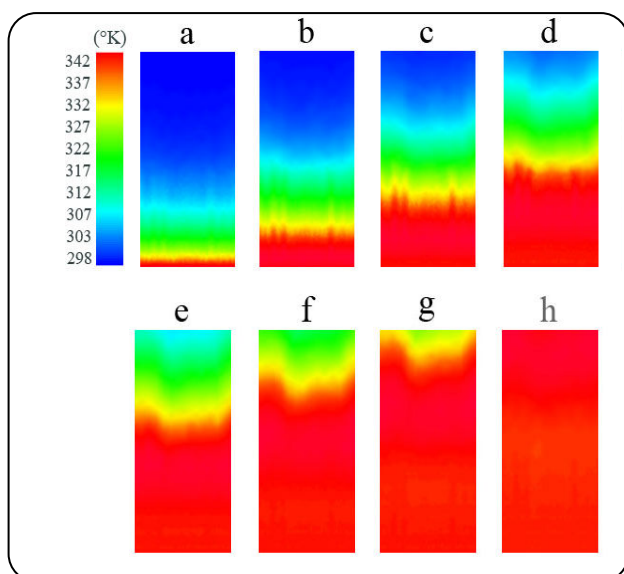


Fig. 3: Contour of total temperature in the case with bed depth 9cm, cube size 4mm and inlet air temperature 70°C at time steps: a) $t=0.1s$, b) $t=0.2s$, c) $t=0.3s$, d) $t=0.4s$, e) $t=0.5s$, f) $t=0.6s$, g) $t=0.7s$ and h) $t=0.8s$.

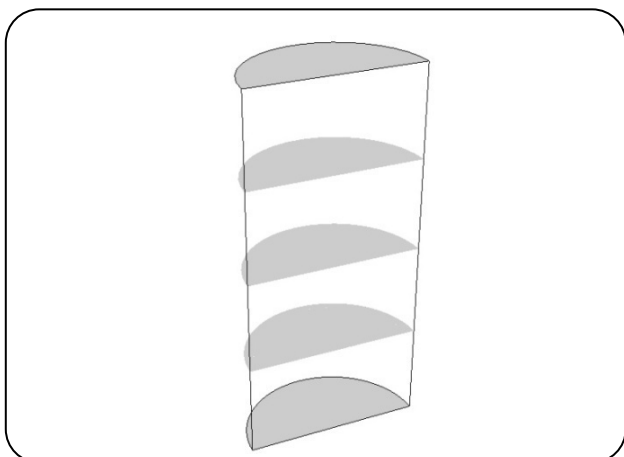


Fig.4: Drying chamber divided to 5 layers by iso-surfaces.

move from the center of carrot toward its surface, therefore during the drying, water content near the carrot surface will increase. Volume fraction contours of water and its vectors obtained from numerical results, are in agreement with the natural process of drying.

With a low flow rate of the upward passed air through bed particles, a fixed bed will be the result. An increase in flow rate causes expanded bed particles and provides a minimal fluidized bed. In the carrot cubes with high initial moisture content, only the top layer of the bed is movable. The bottom layers remain expanded with negligible motion due to dominant cohesive forces exerted by wetted surfaces. In minimum fluidization condition, the pressure drop across the cubic carrot layer was reached the equivalent of the weight of particles in the bed divided by the area of the bed, in other words the frictional force between particles and air, counterbalanced the weight of the particles. As can be seen in Fig. 7 around a carrot cube in the fluidized bed, the boundary layer next to the upper surface of the carrot became thicker and then separated from the surface because of air viscosity. This separation of the boundary layer caused turbulent eddies within which energy was dissipated and which created an upward force on the particle known as form drag. The total force acting on the particle because of the air flow is then the sum of form drag and the viscous drag over the surface. Fig. 7 (a) shows the velocity vectors of air and viscous drag in the sides of a single carrot cube in the fluidized bed and the turbulent eddies in the top of the particle. Fig. 7 (b) shows the pressure contour. As it can be seen from the figure, there is a pressure drop across the single particle due to created eddies.

Results have been analyzed using Taguchi technique to rank factors that can affect the energy utilization ratio in a fluidized bed dryer. As Table 6 represents between factors listed in Table 3, bed depth and inlet air temperature have the maximum interaction. Cube size - inlet air temperature and bed depth - cube size are the other pairs that the interaction between them is significant.

ANOVA is a method that most widely used for determining significant parameters on response by the decomposition of total variation into its appropriate components and measuring their relative effects. The results of ANOVA are shown in Table 7.

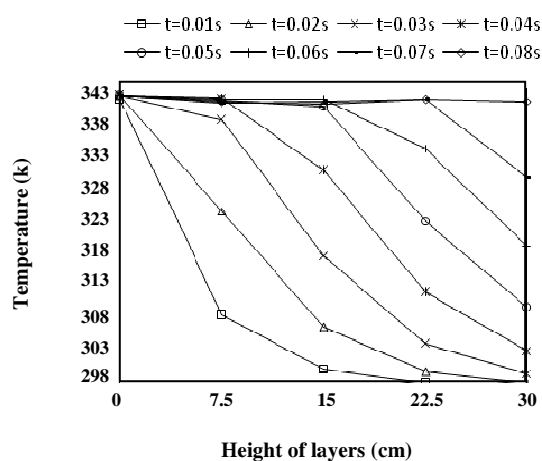


Fig. 5: Variations of temperature versus time and surface position in bed depth 9cm, cube size 4mm and inlet air temperature 70°C.

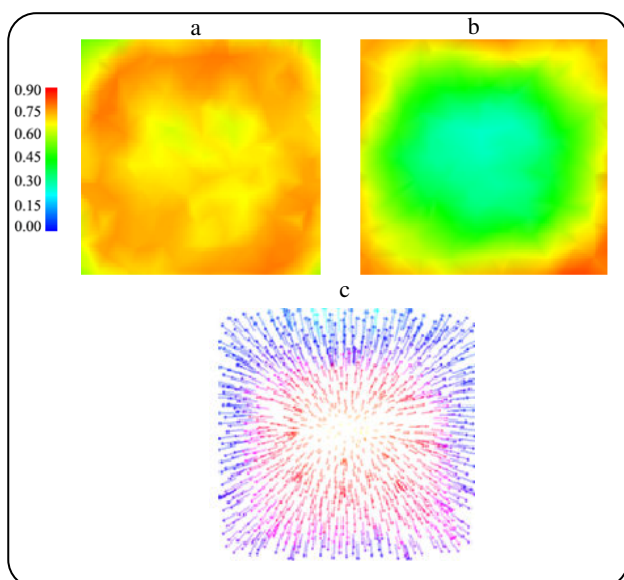


Fig. 6: Volume fraction of water inside a carrot cube after (a) 0.01 s and (b) 0.07 s, (c) water vectors inside the carrot.

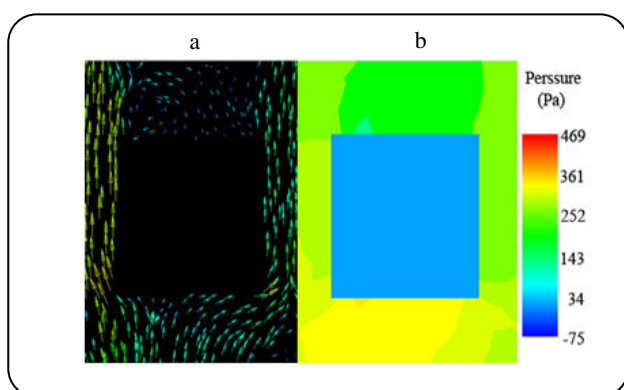


Fig. 7: (a) velocity vectors, and (b) contour of total pressure around a single carrot in the fluidized bed dryer.

Degree of freedom (DOF) for a factor is shown in second column of the ANOVA table and it is defined as:

$$\text{DOF} = n - 1 \quad (24)$$

The sum of squares (S) in the third column of Table 7 for each factor is defined as:

$$S = \sum_{j=1}^n n \cdot (m_j - m_i)^2 \quad (25)$$

The variance and percent of contribution of each factor is calculated as:

$$V_a = \frac{S}{\text{DOF}} \quad (26)$$

$$\text{Percent} = \frac{S}{\text{DOF} \times \sum_{i=1}^N \frac{S}{\text{DOF}}} \times 100 \quad (27)$$

The review of the 'Percent' column shows that the cube size factor contributed the highest percentage to the factor effects.

The averages of energy utilization ratio for all factors at each level were plotted in Fig. 8. From the highest value of average effects for each factor the best level can be determined. According to these figures level 3 of bed depth, level 1 of carrot cube size and level 3 of inlet air temperature can be obtained as the optimum condition.

The levels that cause maximum energy utilization ratio are listed in Table 8. Based on Taguchi technique the expected energy utilization ratio, which is the sum of the total contribution from all factors and the grand average value is 0.203. The different between the grand average value and the average effect of each factor correspond to its optimum level is contribution of each factor. The expected value should get when optimum conditions are applied.

The confirmation test is final and crucial step which is highly recommended by Taguchi to verify the conclusions [9]. In the stage of confirmation experiment, an extra simulation has been performed using the optimum conditions and obtained result were compared with the expected result at optimum condition (Table 8). The confidence interval of energy utilization ratio for this simulation was ± 0.033 and it was within the 95% confidence level of the predicted optimal values. It means that prediction of Taguchi method is reliable.

Table 6: Interaction between factors.

Interaction factor pairs	Interaction severity index
A-C	38.98
B-C	19.04
A-B	10.11

Table 7: ANOVA analysis.

Factor	Degree of freedom (DOF)	Sum of squares (S)	Variance (V)	F-ratio (F)	Pure sum (S')	Percent P (%)
A: Bed depth	2	0.001	0	2.475	0.001	5.438
B: Cube size	2	0.015	0.007	19.911	0.014	69.707
C: Inlet air temperature	2	0.002	0.001	3.742	0.002	10.11
Other / error	2	0.003				14.745
Total	8	0.021				100

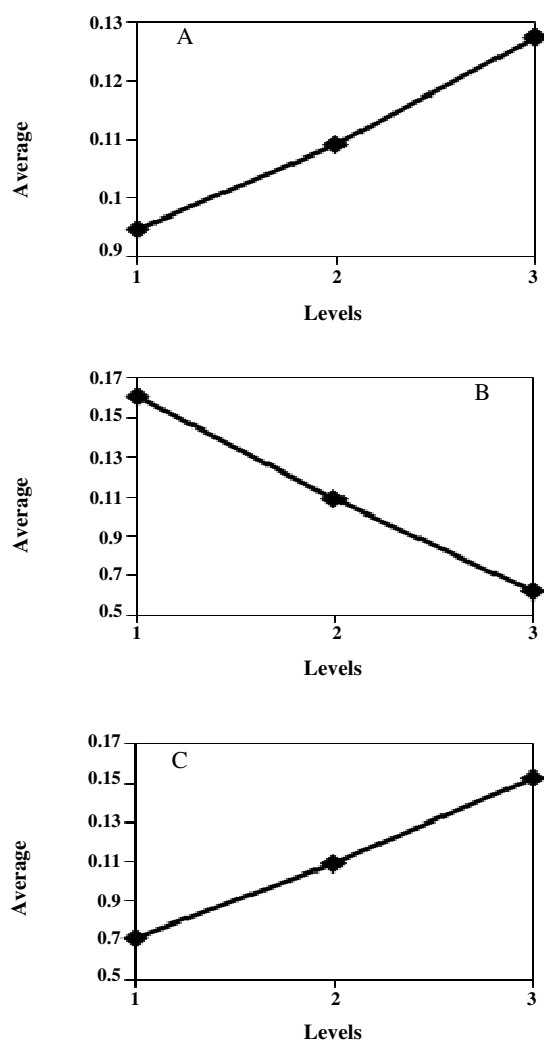


Fig.8: Average effects of factors for each level (A) Bed depth, (B) Cube size, and (C) Inlet air temperature.

In order to validate the simulation results, three experimental tests were done [34]. Before each experiment, the cylindrical drying chamber was filled with square-cubed carrots to a chosen height and then samples were taken out from the cylinder to determine the initial weight. After the dryer was reached at steady state conditions for operation temperatures and fluidization velocities, the carrot cubes were put in the drying chamber and dried there.

Numerical and experimental results have been compared to each other. The outlet air temperature was compared between numerical and experimental data. Tests have been performed for carrot cubes 7mm, bed depth 6cm, and inlet air temperatures 50, 60 and 70°C in the laboratorial fluidized bed dryer. The results were compared with numerical data performed in the same conditions and it has been shown in Fig. 9. Outlet air velocity in both experiments and simulations were also compared to each other, and numerical results were in good agreement with experimental data.

CONCLUSIONS

A laboratorial fluidized bed dryer for drying of carrot cubes was simulated by CFD method and the effect of different parameters such as inlet air temperature, cube size and bed depth on energy utilization ratio at three levels were investigated using Taguchi technique. Among the factors studied, percent contribution of carrot cube size is more significant than other factors, and the pair bed depth-inlet air temperature has the maximum

Table 8: Estimation of the optimum condition (maximum energy utilization ratio).

Factor	Level	Contribution
Bed depth	3	0.018
Cube size	1	0.052
Drying temperature	3	0.022
Total contribution from all factors		0.091
Current grand average of performance		0.111
Expected result at optimum condition		0.203

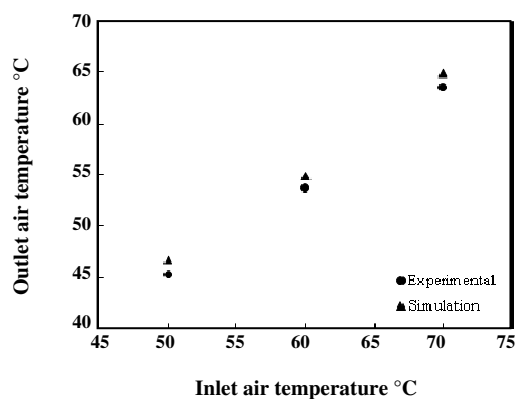


Fig. 9: Comparison of simulation and experimental data at bed depth 6cm, cube size 7mm and inlet air temperature 50 °C, 60 °C and 70 °C.

interaction on each other. It was concluded that this method could be a good way to optimize energy consumption and reduction of losses and costs due to control the parameters. The numerical results show that smaller particle size, deeper bed and higher inlet air temperature increase energy utilization and decrease energy losses from outlet air. Numerical results have been evaluated by comparing with experimental data in terms of outlet air temperature and velocity.

Acknowledgement

The authors would like to acknowledge the University of Tehran for financial support of this research.

Nomenclatures

A	Surface area, m ²
C _p	Specific heat, J/(kg.K)
D _{eff}	Water effective diffusivity, m ² /s
DOF	Degree of freedom
e	Environment
h	Specific enthalpy, J/kg

I	unit tensor
J _j	Diffusion flux of species j, mol/m ² .s
\vec{J}_w	Water mass flux
k _{eff}	Effective conductivity, W/m.K
m _j	Standard average of the results at level j for each factor, unit of the factor
m _t	Total standard average (grand average)
\dot{m}	Mass flow rate, kg/s
n	Total number of levels
N	Number of factors
p	Static pressure, Pa
P	Atmospheric pressure, Pa
P _{vs}	Saturated pressure, Pa
S _h	Heat source, W/m ³
t	Time, s
T	Drying air temperature, K
T _∞	Ambient temperature, K
Y _j	Mass fraction of species j
φ	Relative humidity of air, kg/m ³
μ	Dynamic viscosity, Pa s
ρ	Fluid density, kg/m ³
ρ \vec{g}	Gravitational body force, kg m/s ²
σ _k	Turbulent Prandtl number for k
σ _ε	Turbulent Prandtl number for ε
$\bar{\tau}$	Stress tensor, N/m ²

Superscript

da	Drying air
dc	Drying chamber
a	Air
o	Output
i	Input

Received : Apr. 25, 2011 ; Accepted : Jun. 8, 2013

REFERENCES

- [1] Sumnu G., Turabi E., Oztop M., Drying of Carrots in Microwave and Halogen Lamp Microwave Combination Ovens, *Lebensmittel Wisst- Food Science and Technology*, **38**, p. 549 (2005).
- [2] Kaya A., Aydın O., Demirtas C., Experimental and Theoretical Analysis of Drying Carrots, *Desalination*, **237**, p. 285 (2009).
- [3] Hatamipour M.S., Mowla D., Shrinkage of Carrots During Drying in an Inert Medium Fluidized Bed, *Journal of Food Engineering*, **55**, p. 247 (2002).
- [4] Bialobrzewski I., Zielinska M., Mujumdar A.S., Markowski M., Heat and Mass Transfer During Drying of a Bed of Shrinking Particles Simulation for Carrot Cubes Dried in a Spout-Fluidized-Bed Drier, *International Journal of Heat and Mass Transfer*, **51**, p. 4704 (2008).
- [5] Mujumdar A.S., "Hand Book of Industrial Drying", 3rd Ed, Marcel Dekker, New York (2006).
- [6] Syahrul S., Hamdullahpur F., Dincer I., Exergy Analysis of Fluidized Bed Drying of Moist Particles, *Exergy, an International Journal*, **2**, p. 87 (2002).
- [7] Tiza C., Liasakis G., "Extraction Optimization in Food Engineering", Marcel Dekker, New York (2003).
- [8] Simpson R., Almonacid S., López D., Abakarov A., Optimum Design and Operating Conditions of Multiple Effect Evaporators: Tomato Paste, *Journal of Food Engineering*, **89**, p. 488 (2008).
- [9] Taguchi G., Yokoyama Y., Wu Y., "Taguchi Methods/Design of Experiments", American Supplier Institute (ASI) Press, Tokyo, Japan (1993).
- [10] Mousavi S.M., Jafari A., Chegini S., Turunen I., CFD Simulation of Mass Transfer and Flow Behaviour Around a Single Particle in Bioleaching Process, *Process Biochemistry*, **44**, p. 696 (2009).
- [11] Jafari A., Zamankhan P., Mousavi S.M., Pietarinen K., Modeling and CFD Simulation of Flow Behavior and Dispersivity Through Randomly Packed Bed Reactors, *Chemical Engineering Journal*, **144**, p. 476 (2008).
- [12] Semnani Rahbar M., Alizadeh Dakhel A., Pressure Drop Prediction in Fluidized Bed Dryer of Sodium Perborate Using Computational Fluid Dynamics, *Iran. J. Chem. Chem. Eng.*, **28** (2), p. 33 (2009).
- [13] Gorji M., Bozorgmehry Bozzarjomehry R., Kazemeini M., CFD Modeling of Gas-Liquid Hydrodynamics in a Stirred Tank Reactor, *Iran. J. Chem. Chem. Eng.*, **26** (2), p. 85 (2007).
- [14] Irani M., Bozorgmehry Bozzarjomehry R., Pishvaie S.M.R., Investigating the Effects of Mass Transfer and Mixture Non-Ideality on Multiphase Flow Hydrodynamics Using CFD Methods, *Iran. J. Chem. Chem. Eng.*, **29** (1), p. 51 (2010).
- [15] Alamprese C., Datei L., Semeraro Q., Optimization of Processing Parameters of a Ball Mill Refiner for Chocolate, *Journal of Food Engineering*, **83**, p. 629 (2007).
- [16] Corzo O., Bracho N., Va'squez A., Pereira A., Optimization of a Thin Layer Drying Process for Coroba Slices, *Journal of Food Engineering*, **85**, p. 372 (2008).
- [17] Erbay Z., Icier F., Optimization of Hot Air Drying of Olive Leaves Using Response Surface, *Journal of Food Engineering*, **91** (4), p. 533 (2009).
- [18] Hodali R., Bougard J., Integration of Desiccant Unit in Crops Solar Drying Installation: Optimization by Numerical Simulation, *Energy Conversion and Management*, **42**, p. 1543 (2001).
- [19] Oztop M.H., Sahin S., Sumnu G., Optimization of Microwave Frying of Potato Slices by Using Taguchi Technique, *Journal of Food Engineering*, **79**, p. 83 (2007).
- [20] SrinivasaRao P., Bal B., Goswami T.K., Modelling and Optimization of Drying Variables in Thin Layer Drying of Parboiled Paddy, *Journal of Food Engineering*, **78**, p. 480 (2007).
- [21] Souza J.S., Medeiros M.F.D., Magalhaães M.M.A., Rodrigues S., Fernandes, F.A.N., Optimization of Osmotic Dehydration of Tomatoes in a Ternary System Followed by Air-Drying, *Journal of Food Engineering*, **83**, p. 501 (2007).
- [22] Tasirin S.M., Kamarudin S.K., Ghani J.A., Lee K.F., Optimization of Drying Parameters of Bird's Eye Chilli in a Fluidized Bed Dryer, *Journal of Food Engineering*, **80**, p. 695 (2007).
- [23] Uysal N., Sumnu G., Sahin S., Optimization of Microwave-Infrared Roasting of Hazelnut, *Journal of Food Engineering*, **90** (2), p. 255 (2009).
- [24] Volpato G., Michielin E.M.Z., Ferreira S.R.S., Petrus JCC, Optimization of the Chicken Breast Cooking Process, *Journal of Food Engineering*, **84**, p. 576 (2008).

- [25] Zomorodian A., Zare D., Ghasemkhani H., Optimization and Evaluation of a Semi Continuous Solar Dryer for Cereals (Rice, etc), *Desalination*, **209**, p. 129 (2007).
- [26] Aghbashlo M., Kianmehr M.H., Arabhosseini A., Energy and Exergy Analyses of Thin Layer Drying of Potato Slices in a Semi-Industrial Continuous Band Dryer, *Drying Technology*, **26**, p. 1501 (2008).
- [27] Syahrul S., Dincer I., Hamdullahpur F., Thermodynamic Modeling of Fluidized Bed Drying of Moist Particles, *International Journal of Thermal Sciences*, **42**, p. 691 (2003).
- [28] Ceylan I., Aktas M., Dogan H., Energy and Exergy Analysis of Timber Dryer Assisted Heat Pump, *Applied Thermal Engineering*, **27**, p. 216 (2007).
- [29] Corzo O., Bracho N., Vasquez A., Pereira A., Energy and Exergy Analyses of Thin Layer Drying of Coroba Slices, *Journal of Food Engineering*, **86**, p. 151 (2008).
- [30] Topic R, Mathematical Model for Exergy Analysis of Drying Plants, *Drying Technology*, **13** (1-2), p. 437 (1995).
- [31] Akpınar E.K., Energy and Exergy Analyses of Drying of Red Pepper Slices in Convective Type Dryer, *International Journal of Heat and Mass Transfer*, **31** (8), p. 1165 (2004).
- [32] Akpınar E.K., Midilli A., Bicer Y., Energy and Exergy of Carrots Drying Process via Cyclone Type Dryer, *Energy Conversion and Management*, **46** (15/16), p. 2530 (2005).
- [33] Akpınar E.K., Midilli A., Bicer Y., The First and Second Law Analyses of Thermodynamic of Pumpkin Drying Process, *Journal of Food Engineering*, **72** (4), p. 320 (2006).
- [34] Nazghelichi T., Kianmehr M.H., Aghbashlo M., Thermodynamics Analysis of Fluidized Bed Drying of Carrot Cubes, *Energy*, **35** (12), p. 4679 (2010).